

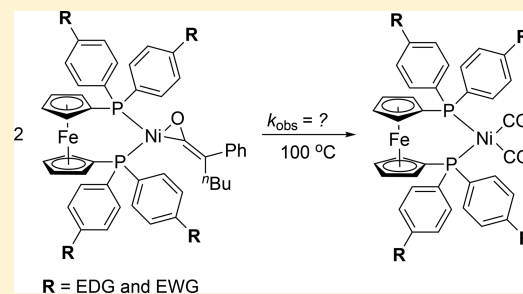
# Electronic Effect of Ligands on the Stability of Nickel–Ketene Complexes

Noman Al, Ryan M. Stolley, Nicholas D. Staudaher,<sup>‡</sup> Ryan T. Vanderlinden, and Janis Louie<sup>\*†</sup>

Department of Chemistry, The University of Utah, 315 S. 1400 E, Rm. 2020, Salt Lake City, Utah 84112, United States

## Supporting Information

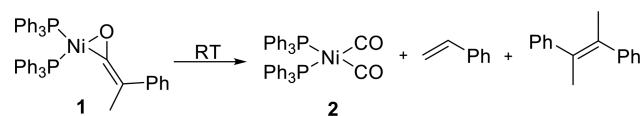
**ABSTRACT:** Electronically variant (dppf)Ni(ketene) complexes were synthesized and characterized to perform kinetic analysis on their decomposition through a decarbonylation/disproportionation process to Ni–CO complexes and alkenes. Ligands containing electron-donating groups stabilized such complexes, whereas an electron-withdrawing group was found to destabilize them. Hammett analysis on the decomposition reaction revealed the buildup of negative charges in the rate-determining step, which corroborates past computational models.



## INTRODUCTION

Despite a long history of coordination complexes of heterocumulenes, Ni–ketene complexes are often overlooked in the field of organometallics. Literature reports of these compounds are limited,<sup>1</sup> primarily owing to their instability and rapid decomposition via decarbonylation.<sup>2</sup> Generally, insufficient reactivity between potential transition metal catalysts and ketenes is not the problem, as ketenes readily form  $\eta^2$ -complexes with various metals (Ni, Pd, Pt, Co, Rh, Ir, etc.).<sup>3</sup> The inability of these  $\eta^2$ -complexes to undergo further useful reactions lies in their propensity to decarbonylate and form stable, unreactive 18-electron carbonyl complexes (2).<sup>4</sup> Carbonyls, being good  $\pi$ -acceptor ligands, also hinder further reactivity by forming strong Ni–CO bonds<sup>5</sup> as products of the decarbonylation process (Scheme 1). In addition, ketenes

### Scheme 1. Decarbonylation of the Ni–Ketene Complex<sup>1</sup>

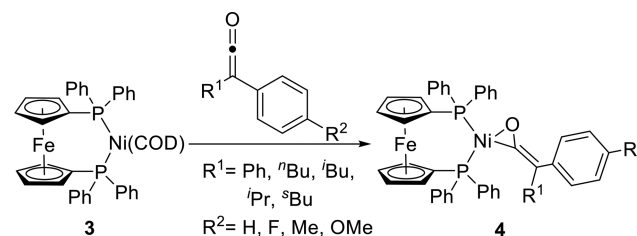


often undergo homodimerization under thermal conditions,<sup>6</sup> limiting the effective concentrations of ketene to generate Ni–ketene complexes. Despite these pitfalls, several nickel-mediated reactions utilizing ketenes directly or containing proposed Ni–ketene complex intermediates are known.<sup>7</sup> These results suggest certain Ni–ketene complexes may actually be quite robust, yet still reactive. This potential to generate such Ni–ketene complexes has inspired us to investigate what factors govern both the stability as well as the reactivity of Ni–ketene complexes.

Past efforts from our research group have led to a synthesis of stable and isolable Ni–ketene complexes using various ketenes and chelating 1,1'-bis(diphenylphosphino)ferrocene

(dppf) as the ligand (Scheme 2).<sup>8</sup> Key to the stability of these complexes versus previous complexes is the more robust

### Scheme 2. Synthesis of (Dppf)Ni(Ketene) Complexes<sup>8</sup>



ligation of a chelating ligand compared to that of the previously used monodentate phosphines.

Kinetic analysis on the thermal decomposition of (dppf)-Ni(ketene) complexes (4) has shown that ketenes appended with electron-donating moieties further stabilized the complexes by resisting the formation of the catalytically inert nickel carbonyl complex.<sup>8</sup> DFT modeling on the mechanism of decomposition revealed a buildup of negative charges on the  $\beta$  carbon of the ketene moiety during the rate-determining step (TS2, Figure 1). The presence of an electron-donating ketene can destabilize the buildup of this negative charge, which lends to the observed stability.

With the electronic effects of the ketenes on the stability of their respective Ni–ketene complexes previously elucidated, we hypothesize that, in a similar manner, electron-donating chelating phosphines would also stabilize such complexes. By increasing the electron density on the nickel center through a highly donating ligand, the buildup of negative charge that occurs during the rate-determining step (RDS) of the

Received: July 13, 2018

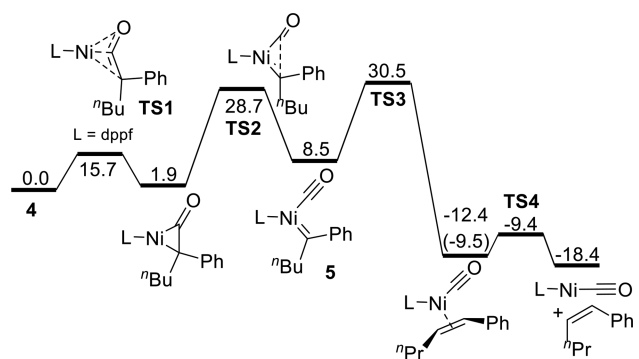


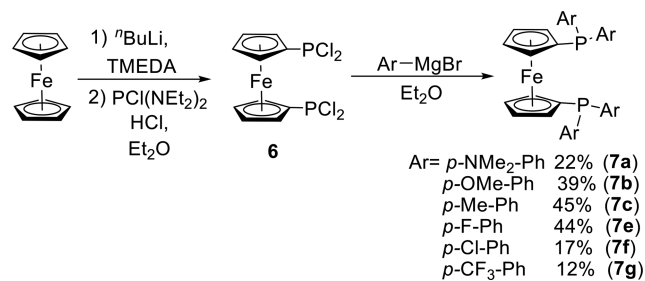
**Figure 1.** DFT modeling of the decomposition of (dppf)Ni(ketene) complexes using BP86/tzvp-svp for optimizations and BLYP/6-31G\* for single-point energies. Number in parentheses corresponds to the *trans*-alkene species.<sup>8</sup>

decarbonylation may be negated, thereby leading to higher stability. The formation of a nickel carbonyl carbene intermediate species (**5**, Figure 1) in the RDS of the decarbonylation can be strongly influenced by the electronic parameter of the ligand. Through Hammett analysis, the electronic effects of the ligand that pertain to the RDS can be obtained, which can be corroborated to stability imparted to the complexes. This would subsequently allow the insight into electronic tuning of the phosphine ligand to increase the stability of Ni–ketene complexes. Ketene-dependent stability on such complexes may also be mitigated, which would further open the possibility of using a variety of ketenes regardless of their electronic nature, a critical property for the general use of Ni–ketene complexes or intermediates. In this report, we present the synthesis of (dppf)–Ni–ketene complexes in which the electronic parameter of the phosphine substituent is systematically varied and perform NMR-based kinetic analysis studies to investigate effects in their rates of decomposition.

## RESULTS AND DISCUSSION

As our group has previously shown, dppf remains the optimal ligand in the synthesis of stable Ni–ketenes complexes. Henceforth, the synthesis of the modified dppf ligands (Scheme 3) was generally carried out via modified literature

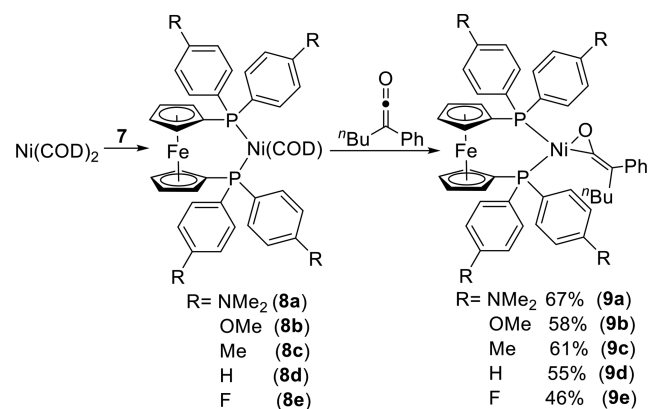
### Scheme 3. Synthesis of Substituted Dppf Ligands<sup>9</sup>



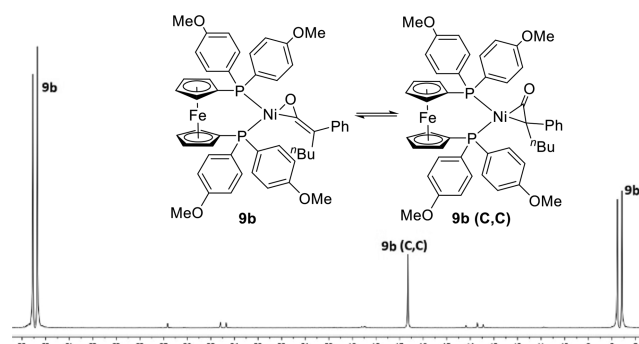
procedures<sup>9</sup> to generate common intermediate **6**, which was treated with the appropriate Grignard reagent to afford the ligands in moderate to high yields (**7a–g**).

The corresponding Ni–ketene complexes were obtained by reaction with Ni(COD)<sub>2</sub> and variable molar equivalents of phenyl *n*-butyl ketene (Scheme 4). A higher equivalence of ketene was required to synthesize the electron-withdrawing Ni–ketene complex **9e**. This can be attributed to an electron-

### Scheme 4. Synthesis of (Dppf)Ni(Ketene) Complexes



deficient nickel center, which hinders the lability of the COD ligand, thereby affecting the ketene coordination to the nickel. When ketene is added to an equimolar mixture of a substituted dppf ligand and Ni(COD)<sub>2</sub>, the formation of the Ni–ketene complex is observed as an appearance of two doublets in the <sup>31</sup>P NMR. X-ray crystal structures of the Ni–ketene complexes have shown that a square planar geometry exists around the nickel center, which, along with past Mayer bond analysis,<sup>8</sup> is indicative of a Ni(II) species. The two doublets seen in the <sup>31</sup>P NMR corresponds to the two inequivalent phosphine atoms on the complex. This observation is critical as it is used to gauge the completion of the reaction and to monitor any other coordination modes of the ketene<sup>8</sup> (Figure 2, **9b** C,C) and

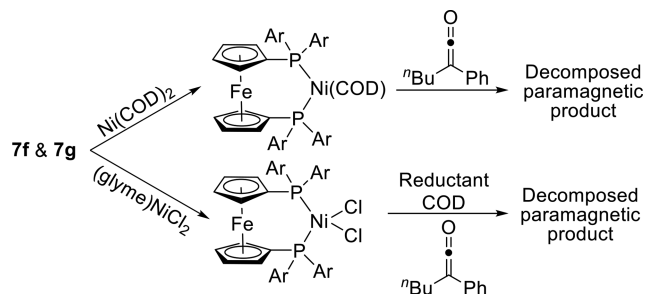


**Figure 2.** <sup>31</sup>P NMR of the formation of **9b**.

undesired products such as possible ketene dimer adducts being formed. Furthermore, the ratio of the two observed coordination modes (C,O and C,C) did not change significantly among the ligands employed in this study.

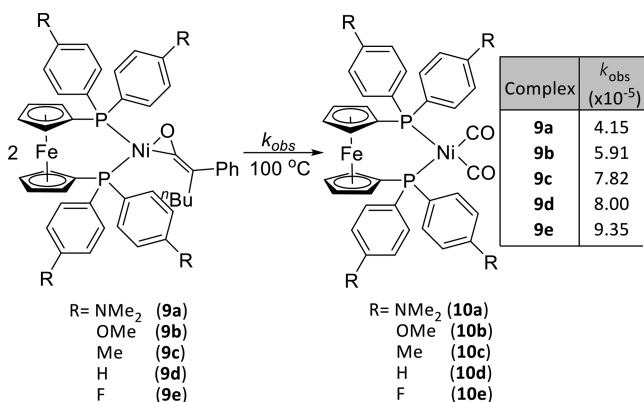
Despite numerous attempts, Ni–ketene complexes containing highly electron-withdrawing substituents such as chloro (**7f**) and trifluoromethyl (**7g**) could not be synthesized. By monitoring through <sup>31</sup>P NMR, we found that the Ni–ketene complexes of these ligands decomposed to unidentifiable paramagnetic products upon the formation of appreciable amounts of the respective ketene complexes. An alternate synthetic pathway using (glyme)NiCl<sub>2</sub> and performing an in situ reduction in the presence of COD and/or ketene was also attempted (Scheme 5). However, repeated trials of this method did not yield the desired product either.

The decomposition of the electronically substituted (dppf)–Ni(ketene) (**9a–e**) complexes to the corresponding (dppf)–Ni(CO)<sub>2</sub> (**9a–e**) complexes was performed by NMR at 100

Scheme 5. Attempted Synthesis of ( $d^{EWG}ppf$ )Ni(Ketene)

$^{\circ}\text{C}$  (Scheme 6) in toluene- $d_8$ . Using 1,3,5-trimethoxybenzene as an internal standard, the relative concentration of the

## Scheme 6. Decomposition of Substituted (Dppf)Ni(Ketene) Complex and Their Observed Rate Constant



complex was monitored upon heating through  $^1\text{H}$  NMR (Figure 3). Over time, the resonances that corresponded to the

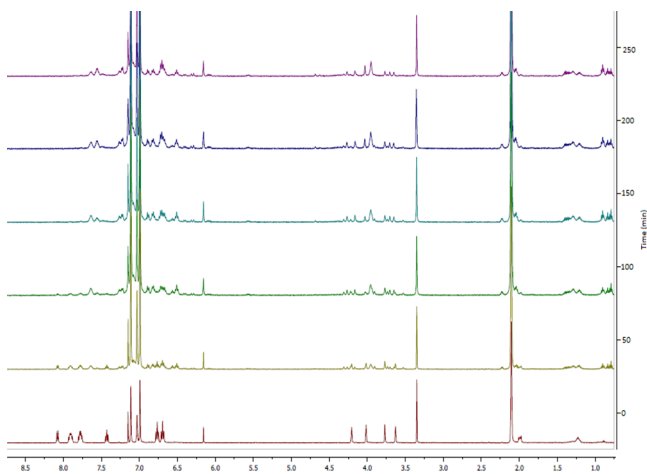


Figure 3.  $^1\text{H}$  NMR of decomposition of 9e, where four singlets in the Cp region ( $3.5\delta$ – $4.25\delta$ ) collapses to two singlets.

Ni–ketene complex decreased and gave rise to resonances that aligned with olefinic protons. The observation of such resonance confirmed that the Ni–ketene complex was decomposing to form olefin byproducts. The decomposition was performed until all of the Ni–ketene complex fully converted to its dicarbonyl counterparts (10).

The data obtained from the kinetic analysis indicate that electronic substitution at the ligand does indeed influence the  $k_{\text{obs}}$  of the decomposition via decarbonylation of Ni–ketene complexes. It revealed that complexes bearing electron-donating dppf (9a–c) demonstrated a  $k_{\text{obs}}$  that is lower than that containing an electronically neutral ligand (9d). Conversely, the complex containing the electron-withdrawing dppf (9e) has a  $k_{\text{obs}}$  that is higher than the neutral species (9d). This highlights the trend that electron-donating phosphines stabilize Ni–ketene complexes, whereas electron-withdrawing phosphines destabilize them. Performing a Hammett analysis on the rate data reveals a positive  $\rho$  value of 1.285, which indicates that the stability of the Ni–ketene complex is strongly influenced by the electronic substituent on the phosphine ligands (Figure 4). The positive slope also corroborates computational studies that indicate negative charge is being built up in the transition state (TS2) during the rate-determining step.

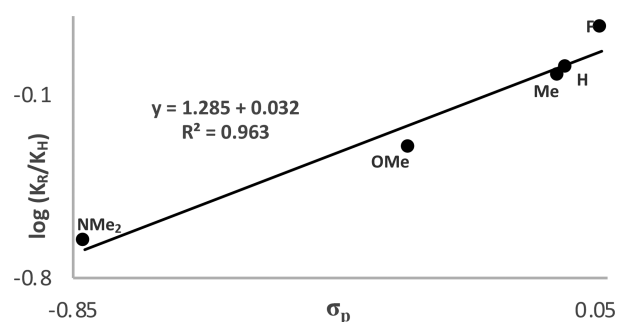


Figure 4. Hammett analysis of the decomposition of the substituted (dppf)Ni(ketene) complex.

The crystal structures obtained for the complexes 9a–e (Figure 5) reveal Ni–O and Ni–C bond lengths that are very similar to each other across the series (Table 1). Additionally,

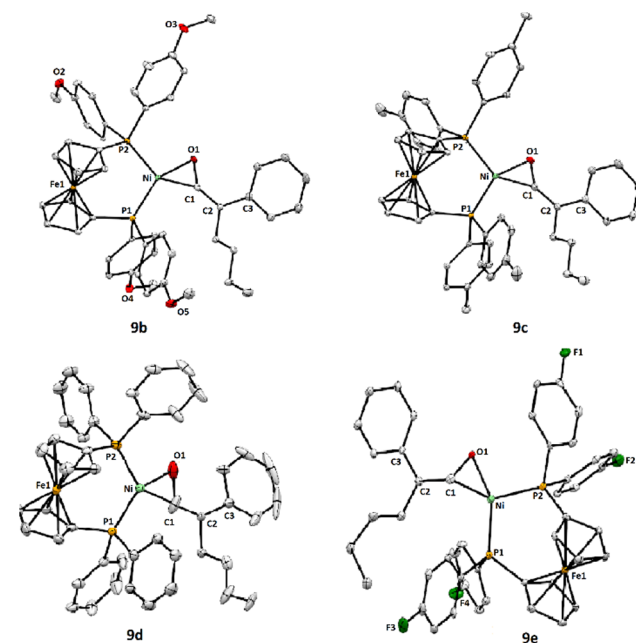


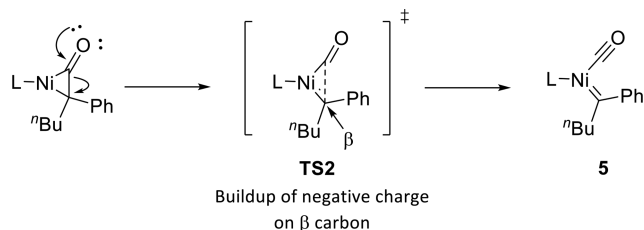
Figure 5. ORTEP diagrams of substituted (dppf)Ni(Ketene) complexes 9b–e. Ellipsoids are set at 30% probability.

Table 1. Selected Bond Lengths (Å), Angles, and Torsions (deg) of (Dppf)Ni(ketene) Complexes

complex	P <sub>1</sub> –Ni	P <sub>2</sub> –Ni	O <sub>1</sub> –Ni	C <sub>1</sub> –Ni	O <sub>1</sub> –C <sub>1</sub>	C <sub>1</sub> =C <sub>2</sub>	O <sub>1</sub> –Ni–C <sub>1</sub>	P <sub>1</sub> –Ni–P <sub>2</sub>	O <sub>1</sub> –C <sub>1</sub> –C <sub>2</sub> –C <sub>3</sub>
9b	2.151	2.225	1.887	1.877	1.265	1.358	39.29	106.53	–2.47
9c	2.155	2.218	1.880	1.872	1.275	1.350	39.73	107.80	–5.26
9d	2.183	2.183	1.862	1.862	1.383	1.291	43.60	108.13	–19.00
9e	2.153	2.232	1.881	1.885	1.284	1.369	39.88	106.16	6.53

the solid-state structure of **9d** was previously found to be disordered, with random orientation of the ketene with respect to the nickel center.<sup>8</sup> In light of these, no discernible correlation between the bond lengths of the metallacycle and their observed rate constant of decomposition can be made. However, the observed electronic trend can be explained using past computational modeling of the decomposition pathway of the Ni–ketene complex. DFT models have shown that the rate-determining step of the decomposition is the formation of the nickel carbonyl complex (**5**). This occurs through a transition state (**TS2**) where a buildup of negative charge on the  $\beta$  carbon occurs, as observed through the Hammett analysis and previous computational studies. When an electronically donating ligand is used (**15a–c**), the nickel center becomes higher in electron density. This causes a resistance for additional electron donation via the carbene formation (Scheme 7). Conversely, the opposite occurs if an

Scheme 7. Ligand Effects on the Rate-Determining Step of the Decomposition of (Dppf)Ni(ketene) Complexes



electron-withdrawing ligand (**9e**) is used, which facilitates the formation of the intermediate **5**, thereby further enabling transformation toward the decomposed product.

## CONCLUSION

Ni–ketene complexes were previously found to be thermally unstable upon isolation, yet they would partake in a variety of reactions, which is indicative of their utilitarian nature. Past research from our group found that the dppf yielded stable derivatives of Ni–ketene complexes, with further studies showing that electron-donating ketenes aid in the stability. In this report, we have demonstrated the electronic effects the phosphine ligands have on the stability of Ni–ketene complexes. NMR-based kinetic analysis on the decomposition of dppf–Ni–ketene complexes with electronically substituted phosphine ligands indicates that ligands bearing electron-donating groups afford stability to the complexes. Meanwhile, phosphine ligands containing an electron-withdrawing group destabilize such complexes, leading to a higher rate of decomposition. Hammett analysis of the data provided insight that the electronic parameters of the phosphine ligand strongly influence the stability, while confirming the buildup on negative charges in the transition state. This information, in conjunction with previous works, presents a more complete profile as to how electronics factor into stabilizing Ni–ketene

complexes. Such complexes which were previously found to be too unstable could potentially be accessed now through the judicious use of electron-donating phosphine ligands. Their characterizations would reveal valuable insight into such complexes, which would allow further probes into their reactivity.

## EXPERIMENTAL SECTION

**General Considerations.** All reactions were carried out under an atmosphere of N<sub>2</sub> in a glovebox or using standard Schlenk techniques. All glassware was oven-dried. Benzene and pentane were sparged with nitrogen, dried over neutral alumina, and deoxygenated over Q5 under N<sub>2</sub> using a Grubbs-type solvent purification system. Dppf, PCl<sub>3</sub>, HCl in ether solution (2 M), <sup>n</sup>BuLi, ferrocene, diethylamine, 4-methoxyphenyl magnesium bromide, 4-fluorophenyl magnesium bromide, 4-methylphenyl magnesium bromide, and 1,3,5-trimethoxybenzene were purchased from Sigma-Aldrich and used without any further purification. Ni(COD)<sub>2</sub> was purchased from Strem and used without any further purification. P(NEt<sub>2</sub>)<sub>2</sub>Cl<sup>10</sup> and phenyl *n*-butyl ketene<sup>11</sup> were prepared according to literature procedure. 4-(Dimethylamino)phenyl magnesium bromide,<sup>12</sup> 4-chlorophenyl magnesium bromide,<sup>13</sup> and 4-(trifluoromethyl)phenyl magnesium bromide<sup>14</sup> were prepared according to literature procedure. Deuterated benzene (Sigma), deuterated toluene, and THF (Cambridge Isotope) were distilled from CaH<sub>2</sub> and degassed by three freeze–pump–thaw cycles. Screw-cap NMR tubes were used for all NMRs. The tubes were cleaned by rinsing with acetone, sonicating with 1:1 THF/concentrated HCl for 1 h to remove residual Ni, and rinsed with water. <sup>1</sup>H NMR spectra were acquired at 500 MHz. <sup>13</sup>C spectra were recorded at 100 or 125 MHz. <sup>31</sup>P spectra were recorded at 121 MHz. All <sup>13</sup>C and <sup>31</sup>P NMR spectra were proton decoupled. <sup>1</sup>H and <sup>13</sup>C spectra were referenced to residual solvent peaks (C<sub>6</sub>D<sub>6</sub>  $\delta$  7.15 and  $\delta$  128.6). <sup>31</sup>P NMR shifts were reported with respect to external 85% H<sub>3</sub>PO<sub>4</sub> (0 ppm). X-ray crystallography data were collected and analyzed.

**Bis(dichlorophosphino)ferrocene (6).** At all times during this reaction, an inert atmosphere of Nitrogen was maintained. To an oven-dried 500 mL RBF with a side arm equipped with a stir bar and a septum was quickly added 2.76 g Ferrocene (14.78 mmol, 1 equiv). The flask was then purged and backfilled 3x under N<sub>2</sub>. Pentane (150 mL) was added, followed by 4.65 mL TMEDA (31 mmol, 2.1 equiv), and 12.42 mL <sup>n</sup>BuLi (31 mmol, 2.1 equiv). This slurry was stirred overnight, after which, an orange color formed. The reaction was cooled to –78 °C, and a solution of P(NEt<sub>2</sub>)<sub>2</sub>Cl (7.16 g, 34.1 mmol, 2.3 equiv) in 20 mL THF was added dropwise. After the addition was completed, the reaction was warmed to room temperature, and left to stir overnight. The reaction was cooled to –78 °C again, and HCl in ether (60.6 mL, 2M, 121.20 mmol, 8.2 equiv) was added dropwise. The reaction was warmed to room temperature and stirred overnight. The following day, the precipitates were filtered out, and the solvent was removed in vacuo. A brown viscous oil was left, to which was added 15 mL of pentane. An orange-yellow solid precipitated out, which was filtered and washed with 2x 5 mL of cold pentane to yield **6** (5.04 g, 88%). NMR of product matches literature values.<sup>15</sup>

**General Procedure for the synthesis of substituted Dppf (7a–g).** At all times during this reaction, an inert atmosphere of nitrogen was maintained. An oven-dried 200 mL RBF with a side arm equipped with a stir bar and septum was purged and backfilled 3x under N<sub>2</sub>. The Grignard reagent (15.47 mmol, 6 equiv) was added via syringe. A solution of **6** (1 g, 2.58 mmol, 1 equiv) in 50 mL of THF

was then added dropwise into the reaction over 10 min. The reaction was left to stir overnight. Water (10 mL) was added, and the organic layer dried using  $\text{MgSO}_4$ , and the solvent removed. The viscous leftover oil was redissolved in minimum diethyl ether, layered with 15 mL of pentane, and left in the freezer at  $-38\text{ }^\circ\text{C}$  overnight. A yellow powder precipitated out, which was filtered and washed with  $3 \times 5$  mL of cold pentane to yield **7a** (412.3 mg, 22%), **7b** (679.4 mg, 39%), **7c** (708.5 mg, 45%), **7e** (710.8 mg, 44%), **7f** (302.1 mg, 17%), and **7g** (255.7 mg, 12%). NMR of product matches literature values.<sup>9</sup>

**General Procedure for Synthesis of Substituted (Dppf)Ni(Ketene) Complexes.** In the  $\text{N}_2$ -filled glovebox,  $\text{Ni}(\text{COD})_2$  (50 mg, 0.182 mmol, 1 equiv) and ligand (**7a–g**) (0.182 mmol, 1 equiv) were weighed into a 20 mL scintillation vial and dissolved in 3 mL of benzene. The solution was stirred for 2 min, at which point ketene was added directly.

**D(NMe<sub>2</sub>)ppf–Ni–Ketene (9a).** Complex **9a** was synthesized according to the general procedure, using **7a** (132.2 mg) and phenyl-*n*-butyl ketene (63.4 mg, 0.36 mmol, 2 equiv). The reaction was left unstirred overnight, and then 15 mL of pentane was layered and left overnight. The solids were filtered and washed  $3 \times$  with 5 mL of pentane and dried under vacuum:  $\delta_{\text{H}}$  (500 MHz,  $\text{C}_6\text{D}_6$ ) 8.47 (2 H, d), 8.21 (4 H, d), 8.19 (4 H, d), 7.49 (2 H, t), 7.04 (1 H, t), 6.50 (4 H, d), 6.46 (4 H, d), 4.57 (2 H, s), 4.15 (2 H, s), 4.03 (2 H, s), 3.83 (2 H, s), 2.42 (12 H, s), 2.32 (12 H, s), 1.46 (2 H, m), 1.37 (2 H, s), 0.69 (2 H, m), 0.63 (3 H, m);  $^{31}\text{P}$  NMR (121 MHz, benzene)  $\delta$  36.37 (d), 12.01 (d);  $^{13}\text{C}$  NMR (500 MHz,  $\text{DMSO-}d_6$ )  $\delta$  161.62 (s), 137.50 (s), 129.12–128.15 (ddd), 127.95 (s), 125.46–125.09 (t), 93.26 (s), 67.48 (s), 55.59 (s), 46.43 (s), 44.76 (s), 34.40 (s), 25.58 (s), 20.70–20.40 (d), 6.33 (s).

**D(OMe)ppf–Ni–Ketene (9b).** Complex **9b** was synthesized according to the general procedure, using **7b** (153.1 mg) and phenyl-*n*-butyl ketene (190.2 mg, 1.09 mmol, 6 equiv). The reaction was left unstirred overnight, and then 15 mL of pentane was layered and left overnight. The solids were filtered and washed  $3 \times$  with 5 mL of pentane and dried under vacuum:  $\delta_{\text{H}}$  (500 MHz,  $\text{C}_6\text{D}_6$ ) 8.38 (2 H, d), 8.09 (8 H, m), 7.49 (2 H, t), 7.05 (1 H, t), 6.72 (8 H, t), 4.40 (2 H, s), 3.98 (2 H, s), 3.92 (2 H, s), 3.78 (2 H, s), 3.23 (6 H, s), 3.11 (6 H, s), 0.87 (6 H, dd,  $J = 9.5, 4.7$  Hz), 0.65 (3 H, d,  $J = 2.9$  Hz);  $\delta_{\text{P}}$  (121 MHz,  $\text{C}_6\text{D}_6$ ) 32.54 (d), 7.75 (d);  $\delta_{\text{C}}$  (500 MHz,  $\text{C}_6\text{D}_6$ ) 160.65 (s), 136.50 (d), 135.94 (d), 134.86 (s), 128.209 (s), 127.966 (d), 127.68 (d), 127.49(d), 126.75 (s), 126.0 (s), 125.22 (s), 114.14 (d), 113.83 (t), 74.07 (s), 70.851 (d), 54.37 (d), 34.061 (s), 29.86 (s), 23.18(s), 22.35 (s), 14.08 (s), 13.91 (s).

**D(Me)ppf–Ni–Ketene (9c).** Complex **9c** was synthesized according to the general procedure, using **7c** (111.0 mg) and phenyl-*n*-butyl ketene (190.2 mg, 1.09 mmol, 6 equiv). The reaction was left unstirred overnight, and then 15 mL of pentane was layered and left overnight. The solids were filtered and washed  $3 \times$  with 5 mL of pentane and dried under vacuum:  $\delta_{\text{H}}$  (500 MHz, toluene- $d_8$ ) 8.17 (2 H, d), 8.08 (4 H, t), 7.94 (4 H, t), 7.41 (2 H, t), 7.14 (1 H, s), 6.96 (4 H, d), 6.89 (4 H, d), 4.40 (2 H, s), 4.00 (2 H, s), 3.84 (2 H, s), 3.75 (2 H, s), 2.09 (6H, s, slight overlap with solvent peak), 1.97 (6 H, s), 1.26 (6 H, m), 0.88 (3 H, t);  $\delta_{\text{P}}$  (121 MHz, toluene- $d_8$ ) 39.96 (d), 14.97 (d);  $^{13}\text{C}$  NMR (500 MHz,  $\text{C}_6\text{D}_6$ )  $\delta$  167.98–167.67 (d), 140.39 (s), 139.91(s), 18.93 (s), 134.96–134.85 (d), 134.41 (s), 134.30 (s), 133.76–133.54 (d), 132.46–132.21 (d), 131.93 (s), 131.50–131.30 (d), 131.19 (s), 129.15 (s), 127.96 (s), 127.87 (s), 127.68 (s), 127.58 (s), 127.48 (s), 127.09 (s), 126.75 (s), 126.04 (s), 125.24 (s), 125.23 (s), 121.33 (s), 85.56 (s), 85.17 (s), 78.62–78.52 (d), 77.80 (s), 76.80 (s), 76.44 (s), 74.36 (s), 73.92 (s), 72.38 (s), 70.92–70.66 (d), 32.55 (s), 32.06 (s), 29.85 (s), 23.13 (s), 22.49–22.35 (d), 20.90–20.80 (d), 14.73 (s), 14.13 (s).

**D(H)ppf–Ni–Ketene (9d).** Complex **9d** was synthesized according to the general literature procedure,<sup>3</sup> using dppf (100.8 mg) and phenyl-*n*-butyl ketene (95 mg, 0.55 mmol, 3 equiv). The reaction was left unstirred overnight, and then 15 mL of pentane was layered and left overnight. The solids were filtered and washed  $3 \times$  with 5 mL of pentane and dried under vacuum. NMR matches those of literature report.<sup>8</sup>

**D(F)ppf–Ni–Ketene (9e).** Complex **9e** was synthesized according to the general procedure, using **7d** (114.0 mg) and phenyl-*n*-butyl ketene (317.1 mg, 1.82 mmol, 10 equiv). The reaction was left unstirred overnight, and then 15 mL of pentane was layered and left overnight. The solids were filtered and washed  $3 \times$  with 5 mL of pentane and dried under vacuum:  $\delta_{\text{H}}$  (500 MHz,  $\text{C}_6\text{D}_6$ ) 8.20 (2 H, d), 7.88 (4 H, q), 7.77 (4 H, q), 7.48 (2 H, d), 7.06 (1 H, t), 6.77 (4 H, t), 6.68 (4 H, t), 4.16 (2 H, s), 3.95 (2 H, s), 3.73 (2 H, s), 3.61 (2 H, s), 2.06 (1 H, m), 1.37 (1 H, m), 0.87 (1 H, t), 0.65 (3 H, t), 0.57 (2 H, m);  $\delta_{\text{P}}$  (121 MHz,  $\text{C}_6\text{D}_6$ ) 39.64 (d), 14.68 (d);  $\delta_{\text{F}}$  (282 MHz,  $\text{C}_6\text{D}_6$ ) 67.47 (s), 67.25 (s);  $^{13}\text{C}$  NMR (500 MHz,  $\text{C}_6\text{D}_6$ )  $\delta$  167.36–167.03 (d), 165.42–167.13 (d), 163.42–163.13 (d), 139.26 (s), 136.87–136.74 (d), 136.18–136.06 (d), 130.40 (s), 130.09 (s), 129.80 (s), 129.47 (s), 127.96 (s), 127.86 (s), 127.77 (s), 127.67 (s), 127.58 (s), 127.48 (s), 127.14 (s), 126.74 (s), 126.03 (s), 125.42 (s), 125.29 (s), 122.01 (s), 115.70–115.23 (d), 84.58 (s), 84.22 (s), 81.11 (s), 78.38 (s), 76.01–75.74 (d), 74.08 (s), 73.991–73.71 (d), 72.73 (s), 70.98 (s), 37.13 (s), 35.03 (s), 32.33 (s), 31.90–31.90 (t), 29.85 (s), 26.62 (s), 23.08 (s), 22.49–2.26 (d), 13.82 (s), 13.49–1.17 (d).

**Kinetic Analyses of the Decomposition of Substituted (Dppf)Ni(Ketene) Complexes.** The procedure was adapted from a previous literature source.<sup>8</sup> In the  $\text{N}_2$ -filled glovebox, the substituted (dppf)Ni(ketene) complex (0.01 mmol) and 1,3,5-trimethoxybenzene (0.008 mmol) standard were measured into a 4 mL scintillation vial with stir bar in the glovebox and dissolved in toluene- $d_8$  (0.75 mL) with vigorous stirring. The solution was then transferred through a pipet filter with glass wool to screw cap NMR tubes and analyzed by  $^1\text{H}$  NMR (500 MHz). The tubes were immersed in a  $100\text{ }^\circ\text{C}$  oil bath for 10 min and cooled to room temperature, and the exterior was cleaned to remove any oil residue and the mixture analyzed again by  $^1\text{H}$  NMR. The heating/NMR cycles were repeated until 25 time points had been obtained. Two kinetic data sets were collected for each complex (Table 2). In some trials, significant line broadening

**Table 2.** Kinetic Analysis Data for the Decomposition of Substituted Ni–Ketene Complexes

complex	$k_{\text{obs}}$ ( $\times 10^{-5}$ )	$R^2$	average $k_{\text{obs}}$
9a	4.15	0.9965	4.15
	4.14	0.9933	
9b	5.90	0.9959	5.91
	5.918	0.9945	
9c	7.89	0.9923	7.82
	7.75	0.99100	
9d	8.00	0.9900	8.00
	7.98	0.9970	
9e	9.39	0.9911	9.35
	9.40	0.9985	

was observed after a few time points. We believe this is due to oxygen contamination through seepage into the NMR tube. Such trials were omitted and repeated with a fresh sample.

## ■ ASSOCIATED CONTENT

### Supporting Information

The Supporting Information is available free of charge on the ACS Publications website at DOI: 10.1021/acs.organomet.8b00484.

NMR spectra and crystallographic data (PDF)

Crystal structure (XYZ)

### Accession Codes

CCDC 1843712–1843714 contain the supplementary crystallographic data for this paper. These data can be obtained free of charge via [www.ccdc.cam.ac.uk/data\\_request/cif](http://www.ccdc.cam.ac.uk/data_request/cif), or by emailing [data\\_request@ccdc.cam.ac.uk](mailto:data_request@ccdc.cam.ac.uk), or by contacting The

Cambridge Crystallographic Data Centre, 12 Union Road, Cambridge CB2 1EZ, UK; fax: +44 1223 336033.

## AUTHOR INFORMATION

### Corresponding Author

\*E-mail: [louie@chem.utah.edu](mailto:louie@chem.utah.edu).

### ORCID

Nicholas D. Staudaher: 0000-0002-5720-0949

Janis Louie: 0000-0003-3569-1967

### Present Address

<sup>‡</sup>Department of Chemistry, The University of Wisconsin, 1101 University Avenue, Madison, WI 53706.

### Notes

The authors declare no competing financial interest.

## ACKNOWLEDGMENTS

We gratefully acknowledge the National Science Foundation (CHE1213774) and the National Institutes of Health (GM076125) for financial support. The authors would like to gratefully acknowledge Andrew Clevenger from the University of Utah for his invaluable insights on Ni–ketene complexes and for discussion and interpretation of kinetics data.

## REFERENCES

- (1) (a) Hoberg, H.; Korff, J. Durch nickel (0) ausgeloste dimerisierung von diphenketen. *J. Organomet. Chem.* **1978**, *152*, C39–C41. (b) Hofmann, P.; Perez-Moya, L. A.; Steigelmann, O.; Riede, J. Eta-2-(C,O) Ketene coordination at nickel(O). Synthesis, bonding, and molecular structure of (dtbpm)Ni[eta-2-(C,O)-Ph<sub>2</sub>C<sub>2</sub>O] [dtbpm = bis(di-tert-butylphosphino)methane]. *Organometallics* **1992**, *11* (3), 1167–1176. (c) Curley, J.; Kitiachvili, K. D.; Waterman, R.; Hillhouse, G. L. Sequential Insertion Reactions of Carbon Monoxide and Ethylene into the Ni-C Bond of a Cationic Nickel (II)Alkyl Complex. *Organometallics* **2009**, *28*, 2568–2571.
- (2) Miyashita, A.; Sugai, R.; Yamamoto, J. Synthesis and reactivities of novel eta-2-(C,O) alkylphenylketene complexes of nickel. Coordination-mode switching reaction of the ketene ligand. *J. Organomet. Chem.* **1992**, *428*, 239–247.
- (3) (a) Grotjahn, D. B.; Collins, L. S. B.; Wolpert, M.; Bikzhanova, G. A.; Lo, H. C.; Combs, D.; Hubbard, J. L. First Direct Structural Comparison of Complexes of the Same Metal Fragment to Ketenes in both C,C- and C,O-Bonding Modes. *J. Am. Chem. Soc.* **2001**, *123*, 8260–8270. (b) Grotjahn, D. B.; Bikzhanova, G. A.; Concolino, T.; Lam, K.; Rheingold, A. L. J.; Collins, L. S. B. Controlled, Reversible, Conversion of a Ketene Ligand to Carbene and CO Ligands on a Single Metal Center. *J. Am. Chem. Soc.* **2000**, *122*, S222–S223. (c) Urtel, H.; Bikzhanova, G. A.; Grotjahn, D. B.; Hofmann, P. Reversible Carbon-Carbon Double Bond Cleavage of a Ketene Ligand at a Single Iridium (I) Center: A theoretical Study. *Organometallics* **2001**, *20*, 3938–3949.
- (4) Ellgen, P. C. Kinetics and mechanism of the reactions of the di.mu.-carbonyl-bis(cyclopentadienyl)dinickel(0) with monodentate ligands. *Inorg. Chem.* **1971**, *10*, 232–239.
- (5) Sunderlin, L. S.; Wang, D.; Squires, R. R. Metal (iron and nickel) carbonyl bond strengths in Fe(CO)<sub>n</sub>- and Ni(CO)<sub>n</sub>-. *J. Am. Chem. Soc.* **1992**, *114*, 2788–2796.
- (6) Hurd, C. D.; Roe, A. S. Ketene and its Dimer. *J. Am. Chem. Soc.* **1939**, *61*, 3355–3359.
- (7) (a) Zhang, Z.; Zhang, Y.; Wang, J. Carbonylation of Metal Carbene with Carbonyl Monoxide: Generation of Ketene. *ACS Catal.* **2011**, *1*, 1621–1630. (b) Ruchardt, C.; Schrauzer, G. N. Über die Carbonylierung von Carbenen und die katalytische Zersetzung von Diazoalkanen mit Nickelcarbonyl. *Chem. Ber.* **1960**, *93*, 1840–1848. (c) Auvinet, A. L.; Harrity, J. P. A Nickel-Catalyzed Benzannulation

Approach to Aromatic Boronic Esters. *Angew. Chem., Int. Ed.* **2011**, *50*, 2769–2772. (d) Huffman, M. A.; Liebeskind, L. S. Nickel(0)-catalyzed synthesis of substituted phenols from cyclobutenones and alkynes. *J. Am. Chem. Soc.* **1991**, *113*, 2771–2772. (e) Kumar, P.; Troast, D. M.; Cella, R.; Louie, J. Ni-Catalyzed ketene cycloadditions: A System that Resists the Formation of Decarbonylation Side Products. *J. Am. Chem. Soc.* **2011**, *133*, 7719–7721. (f) Rofer-DePoorter, C. K. A comprehensive mechanism for the Fischer-Tropsch Synthesis. *Chem. Rev.* **1981**, *81*, 447–474.

(8) Staudaher, N. D.; Arif, A. M.; Louie, J. Synergy between Experimental and Computational Chemistry Reveals the mechanism of Decomposition of Nickel-Ketene Complexes. *J. Am. Chem. Soc.* **2016**, *138*, 14083–14091.

(9) (a) Qin, L.; Hirao, H.; Zhou, J. Regioselective Heck reaction of aliphatic olefins and aryl halides. *Chem. Commun.* **2013**, *49*, 10236–10238. (b) Ogasawara, M.; Takizawa, K.; Hayashi, T. Effects of Bidentate Phosphine Ligands on syn-anti Isomerizations in  $\pi$  Allylpalladium complexes. *Organometallics* **2002**, *21* (22), 4853–4861.

(10) Coyle, E. E.; Doonan, B. J.; Holohan, A. J.; Walsh, K. A.; Lavigne, F.; Krenske, E. H.; O'Brien, C. Catalytic Wittig Reactions of Semi- and Nonstabilized Ylides Enabled by Ylide Tuning. *Angew. Chem., Int. Ed.* **2014**, *53*, 12907–12911.

(11) Staudaher, N. D.; Lovelace, J.; Johnson, M. P.; Louie, J. Preparation of aryl alkyl ketenes. *Organic Syntheses*; John Wiley & Sons, Inc.: Hoboken, NJ, 2018; Vol. 94, pp 1–15.

(12) Zhu, C.; Oliveira, J. C. A.; Shen, Z.; Huang, H.; Ackermann, L. Manganese (II/III/I)-Catalyzed C-H Arylations in continuous Flow. *ACS Catal.* **2018**, *8*, 4402–4407.

(13) Liu, X.; Liang, Y.; Ji, J.; Luo, J.; Zhao, X. Chiral Selenide-catalyzed Enantioselective Allylic reaction and intermolecular Difunctionalization of Alkenes: Efficient Construction of C-SCF<sub>3</sub> Stereogenic Molecules. *J. Am. Chem. Soc.* **2018**, *140*, 4782–4786.

(14) Guha, S.; Kazi, I.; Mukherjee, P.; Sekar, G. Halogen-bonded iodonium ion catalysis: a route to  $\alpha$ -hydroxy ketone via domino oxidations of secondary alcohols and aliphatic C-H bonds with high selectivity and control. *Chem. Commun.* **2017**, *53*, 10942–10945.

(15) Nagahora, N.; Sasamori, T.; Watanabe, Y.; Furukawa, Y.; Tokitoh, N. Kinetically Stabilized 1,1'-Bis[(E)-diphosphenyl]-ferrocenes; Syntheses, Structures, Properties, and Reactivity. *Bull. Chem. Soc. Jpn.* **2007**, *80* (10), 1884–1900.